

Published in final edited form as:

Chem Commun (Camb). 2010 August 14; 46(30): 5542–5544. doi:10.1039/c0cc00423e.

Antibiotic selectivity for prokaryotic vs. eukaryotic decoding sites†

Yun Xie, Andrew V. Dix, and Yitzhak Tor

Department of Chemistry and Biochemistry, University of California, San Diego, La Jolla, CA 92093-0358, USA.

Yitzhak Tor: ytor@ucsd.edu

Abstract

A FRET assembly reports antibiotic affinities to two different RNA targets. A binder was labeled with a fluorophore that acts both as an acceptor for the emissive nucleoside on the bacterial A-site and a donor fluorophore for the terminally-labeled human A-site. Unlabeled drugs were used to dissociate the labeled antibiotic.

The bacterial ribosome is targeted by the majority of diverse and clinically significant antibiotics, of both natural and synthetic origin.^{1,2} The fundamental role and abundance of this translational ribonucleoprotein machinery in every cell make it an obvious target from evolutionary and functional perspectives, but it presents a formidable challenge for the discovery and development of new antibacterials.^{2,3} In particular, the similarity between functional rRNA sites in prokaryotes and eukaryotes as well as between naïve and resistant bacteria could significantly limit the therapeutic potential of new agents. While numerous factors influence the efficacy and adverse effects of any drug, its affinity to competing targets is of fundamental significance. The ability to discern the inherent target selectivity of existing and candidate antibiotics could therefore critically impact the discovery and development of new agents.

Among the most commonly targeted ribosomal sites, the decoding (or A-site) rRNA is of particular significance.⁴ It acts as a conformational switch that gauges codon–anticodon recognition.⁵ Altering its conformational dynamics by bound aminoglycosides, a large family of potent naturally occurring antibiotics, lowers the fidelity of protein synthesis, leading to bacterial cell death.^{5,6} Although several “mutations” distinguish the prokaryotic 16S decoding site from the corresponding eukaryotic 18S sequence (Fig. 1), biochemical and structural studies illustrate their similarity as well as their ability to bind aminoglycosides.⁷ It has also been suggested that the clinical value of aminoglycosides could potentially depend on their ability to differentiate between two closely related targets.^{8,9} We therefore sought out a straightforward approach to determine the selectivity traits of A-site binders. Here we disclose the design and implementation of a FRET-based, three-component assembly that facilitates a rapid determination of the relative affinity of any given binder to the eukaryotic and prokaryotic decoding sites in a single experiment.

To accomplish this task, we have relied on the following components: (1) an aminoglycoside with modest affinity to both the prokaryotic and eukaryotic A-sites (*e.g.*,

†Electronic supplementary information (ESI) available: Experimental details, photophysical data.

kanamycin A), labeled with a small non-perturbing fluorophore (marked **F2**) at a position that is not essential for rRNA binding; (2) a bacterial 16S A-site RNA construct modified with an isomorphous, emissive nucleoside analog (labeled **F1**) at a position proximal to the binding site, but not part of it; and (3) a human 18S A-site rRNA construct labeled at its terminus with a third fluorophore (designated **F3**). To generate unique spectral signatures for each binding event, the following photophysical conditions had to be met: (1) the isomorphous fluorescent probe on the bacterial A-site construct (**F1**) had to exclusively serve as a FRET donor to the fluorophore placed on the aminoglycoside antibiotic (**F2**); and (2) the latter, in turn, had to specifically serve as a FRET donor for the terminal fluorophore on the human A-site (**F3**).

The experiment is conceptually illustrated in Fig. 2. When all three components, the tagged aminoglycoside and the two RNA constructs, are equilibrated together, the presence of the antibiotic on the 16S RNA can be visualized by selectively exciting **F1**, and monitoring the emission of **F2**. The fraction of the ligand bound to the 18S A-site can be visualized by selectively exciting **F2** and detecting the emission of the acceptor **F3**. More importantly, when an unlabeled competitor small-molecule is added to the mixture and displaces the tagged antibiotic from the 16S A-site, the acceptor emission **F2** is lost, while the fluorescence of the donor nucleoside **F1** is recovered. Accordingly, when the “placeholder” tagged antibiotic is displaced from the 18S A-site, the emission of **F2** is recovered, and the sensitized emission of **F3** is lost. Based on the relative changes in these spectral signatures, measured in one cuvette by following two different emission spectra, the affinity and selectivity of any candidate antibiotic can be determined, as it displaces the tagged ligand on the two related A-sites, according to its inherent selectivity.

The selection of the two orthogonal, yet matched, FRET pairs is critical to the success of this experiment. We identified 5-methoxyquinazoline-2,4-(1*H*,3*H*)-dione **F1**, an emissive uracil analogue, serving as a suitable donor for 7-diethylaminocoumarin-3-carboxylic acid **F2** (Fig. 3).¹⁰ We also found that Dy547 **F3** is a fitting acceptor for **F2**. The absorption maximum of **F1** at 320 nm corresponds to a wavelength with a minimal absorbance of **F2**, while the emission of **F1**, centered at 395 nm ($\Phi_F = 0.16$), overlaps perfectly with the absorption band of **F2**, which emits at 473 nm ($\Phi_F = 0.83$) (Fig. 3).¹⁰ The emission of **F2**, in turn, overlaps with the absorption band of **F3**, which exhibits absorption maxima at 516 and 549 nm and emits at 563 nm ($\Phi_F = 0.27$). Importantly, the molar extinction coefficients of **F3** are negligible at the absorption maxima of **F1** and **F2**. The critical Förster radii for the **F1/F2** ($R_0 = 27 \text{ \AA}$) and **F2/F3** ($R_0 = 45 \text{ \AA}$) pairs are apt for the proposed experiments.¹¹ According to previous results¹² and control experiments,¹³ the replacement of U1406 in the 16S A-site by a fluorescent nucleoside does not significantly impact the antibiotic affinity to the model construct.

For competition studies, the two A-site constructs were pre-folded separately, mixed together and then treated with a two-mole equivalent of coumarin labeled kanamycin A (Fig. 4).¹³ Diverse antibiotics were titrated into this mixture of the kanamycin-bound A-sites. These include several aminoglycosides, semisynthetic aminoglycosides, as well as a macrolide, a peptide and an oxazolidinone-based antibiotic (Fig. 4). The relative emissions of all fluorophores were independently recorded. As productive competition on the 16S A-site advances, the emission intensity of the fluorescent nucleobase **F1** increased, while the emission of the coumarin **F2** was lost (Fig. 5).¹³ For the 18S A-site, the emission intensity of the Dy547 **F3** was reduced. Plotting the fractional fluorescence saturation against the concentration of the competitors yields titration curves (Fig. 5).¹³ Table 1 provides the IC_{50} values for both the 16S and 18S A-sites and the selectivity ratio.

In agreement with reported trends, aminoglycoside antibiotics, including neomycin, tobramycin and paromomycin, do not display a dramatic preference for either the bacterial or human A-sites (Table 1).^{7c,9,13–15} Among all aminoglycosides tested, neomycin B is the only antibiotic that displays selectivity for the prokaryotic 16S A-site. Neamine, the core aminoglycosidic pharmacophore, binds quite strongly to the eukaryotic A-site. Its affinity to the latter is comparable to that of neomycin, yet its affinity to the prokaryotic A-site is significantly lower than neomycin's and is comparable to that of tobramycin. Notably, the loss of the neobiosamine moiety from neomycin lowers the preference for the prokaryotic A-site. Two semi-synthetic amino-aminoglycoside derivatives were also tested. Amino-tobramycin and amino-kanamycin A,¹⁶ while displaying higher affinity for both A-sites compared to the parent antibiotics, still prefer the 18S RNA, with amino-kanamycin A displaying a higher 16S/18S selectivity ratio.

Negamycin, a dipeptide antibiotic, is an active bactericidal compound discovered in the 1970s.¹⁷ Interestingly, little is certain about its mode of action. While originally identified as a protein synthesis inhibitor with enhanced miscoding activity, suggestive of A-site binding,¹⁸ a recent crystal structure implied that its bactericidal potency could result from its binding to the wall of the peptide exit tunnel of the large ribosomal subunit.¹⁹ Our data show that negamycin indeed binds both A-sites with affinities similar to that of kanamycin A. Finally, a macrolide (erythromycin), a lincosamide (lincomycin) and an oxazolidinone-based antibiotic (linezolid) showed, as expected, little or no binding to both ribosomal RNA targets (Table 1).

While it is tempting to compare selectivity ratios and apparent antibiotic toxicities, the nature of the latter complicates such correlations. In particular, the diverse organisms, conditions and antibiotics used hinder the development of firm relationships.²⁰ There is, however, a qualitative correlation between the trends observed for aminoglycoside antibiotics (Table 1) and their nephrotoxicity as evaluated in rat models. Paromomycin, while displaying a lower affinity for the 18S A-site compared to neomycin, has a higher histopathology score than neomycin (Fig. S1[†]).^{13,21} This could potentially be explained by its higher preference for the human A-site. Similarly, tobramycin has a five-fold lower affinity for the 18S A-site compared to neomycin, but is more selective for the eukaryotic A-site. These opposing factors could contribute to its low histopathology score, which is similar to that of neomycin.

In summary, we have developed a three-component assembly that facilitates the real-time evaluation of the affinity and selectivity of small-molecules to the bacterial and human ribosomal decoding sites in a single experiment. It relies on two orthogonal FRET pairs that act in concert to generate unique spectral signatures for each binding and displacement event. The wide spectral window spanned by the absorption and emission of the selected chromophores (*ca.* 300–600 nm) and their sequential overlap are facilitated by the use of an isomorphous nucleoside analogue, which provides a short wavelength trigger while maintaining the bacterial RNA fold. In addition to assessing the selectivity traits of known antibiotics, we were able to gather affinity and selectivity data for compounds that are not generally considered to be A-site binders. While we note, naturally, that a multitude of factors contribute to the apparent toxicity of any drug, where target selectivity is just one of them, having a simple tool to screen derivatives prior to advancing them into preclinical evaluation could prove highly valuable.

[†]Electronic supplementary information (ESI) available: Experimental details, photophysical data.

Supplementary Material

Refer to Web version on PubMed Central for supplementary material.

Acknowledgments

We thank the National Institutes of Health (GM 069773) for support and the National Science Foundation (instrumentation grants CHE-9709183 and CHE-0741968). We are grateful to Drs Yuzuru Akamatsu and Yoshikazu Takahashi for a generous gift of negamycin and to Dr Keiichi Ajito for helpful discussions.

Notes and references

1. Gale, EF.; Cundliffe, E.; Renolds, PE.; Richmond, MH.; Waring, MJ. *The Molecular Basis of Antibiotic Action*. London: John Wiley & Sons; 1981. Green R, Noller HF. *Annu. Rev. Biochem* 1997;66:679–716. [PubMed: 9242921] Puglisi, JD.; Blanchard, SC.; Dahlquist, KD.; Eason, RG.; Fourmy, D.; Lynch, SR.; Recht, MI.; Yoshizawa, S. *The Ribosome: Structure, Function, Antibiotics, and Cellular Interactions*. Garrett, RA.; Douthwaite, SR.; Liljas, A.; Matheson, AT.; Moore, PB.; Noller, HF., editors. Washington D.C: ASM Press; 2000. p. 419-429.
2. Yonath A. *Annu. Rev. Biochem* 2005;74:649–679. [PubMed: 16180279]
3. Wimberly BT. *Curr. Opin. Investig. Drugs* 2009;10:750–765.
4. Gallego J, Varani G. *Acc. Chem. Res* 2001;34:836–843. [PubMed: 11601968] Tor Y. *ChemBioChem* 2003;4:998–1007. [PubMed: 14523917] Sutcliffe JA. *Curr. Opin. Microbiol* 2005;8:534–542. [PubMed: 16111914] Hermann T. *Biochimie* 2006;88:1021–1026. [PubMed: 16872733] Tor Y. *Biochimie* 2006;88:1045–1051. [PubMed: 16581175]
5. Carter AP, Clemons WM, Brodersen DE, Morgan-Warren RJ, Wimberly BT, Ramakrishnan V. *Nature* 2000;407:340–348. [PubMed: 11014183] Ogle JM, Brodersen DE, Clemons WM Jr, Tarry MJ, Carter AP, Ramakrishnan V. *Science* 2001;292:897–902. [PubMed: 11340196] Vicens Q, Westhof E. *Structure* 2001;9:647–658. [PubMed: 11587639]
6. Schlunzen F, Zarivach R, Harms J, Bashan A, Tocilj A, Albrecht R, Yonath A, Franceschi F. *Nature* 2001;413:814–821. [PubMed: 11677599] Vicens Q, Westhof E. *ChemBioChem* 2003;4:1018–1023. [PubMed: 14523919] Francois B, Russell RJM, Murray JB, Aboul N, Masquida B, Vicens Q, Westhof E. *Nucleic Acids Res* 2005;33:5677–5690. [PubMed: 16214802] Kaul M, Barbieri CM, Pilch DS. *J. Am. Chem. Soc* 2006;128:1261–1271. [PubMed: 16433544]
7. (a) Recht MI, Douthwaite S, Puglisi JD. *EMBO J* 1999;18:3133–3138. [PubMed: 10357824] (b) Lynch SR, Puglisi JD. *J. Mol. Biol* 2001;306:1037–1058. [PubMed: 11237617] (c) Kaul M, Barbieri CM, Pilch DS. *J. Mol. Biol* 2005;346:119–134. [PubMed: 15663932] (d) Hobbie SN, Kalapala SK, Akshay S, Bruell C, Schmidt S, Dabow S, Vasella A, Sander P, Böttger EC. *Nucleic Acids Res* 2007;35:6086–6093. [PubMed: 17766247]
8. Hobbie SN, Akshay S, Kalapala SK, Bruell CM, Shcherbakov D, Böttger EC. *Proc. Natl. Acad. Sci. U. S. A* 2008;105:20888–20893. [PubMed: 19104050]
9. (a) Ryu DH, Rando RR. *Bioorg. Med. Chem* 2001;9:2601–2608. [PubMed: 11557348] (b) Wong C, Hendrix M, Priestley ES, Greenberg WA. *Chem. Biol* 1998;5:397–406. [PubMed: 9662506]
10. Xie Y, Dix AV, Tor Y. *J. Am. Chem. Soc* 2009;131:17605–17614. [PubMed: 19908830]
11. Based on crystal structures (PDB 2ESI, 1FYO, and 1FYP), the estimated distance between **F1** and **F2** is less than 10 Å, while the distance between **F2** and **F3** is less than 20 Å.
12. Srivatsan SG, Tor Y. *J. Am. Chem. Soc* 2007;129:2044–2053. [PubMed: 17256858]
13. See supporting information for additional details.
14. Griffey RH, Hofstalter SA, Sannes-Lowery KA, Ecker DJ, Croke ST. *Proc. Natl. Acad. Sci. U. S. A* 1999;96:10129–10133. [PubMed: 10468574]
15. Few studies have examined aminoglycoside affinity to both A-sites under identical experimental conditions.
16. Wang H, Tor Y. *Angew. Chem., Int. Ed* 1998;37:109–111.

17. Mizuno S, Nitta K, Umezawa H. *J. Antibiot* 1970;23:581–588. [PubMed: 4950815] Kondo S, Shibahara S, Takahashi S, Maeda K, Umezawa H, Ohno M. *J. Am. Chem. Soc* 1971;93:6305–6306. [PubMed: 5121145]
18. Arakawa M, Shiozuka M, Nakayama Y, Hara T, Hamada M, Kondo SI, Ikeda D, Takahashi Y, Sawa R, Nonomura Y, Sheykholeslami K, Kondo K, Kaga K, Kitamura T, Suzuki-Miyagoe Y, Takeda SI, Matsuda R. *J. Biochem* 2003;134:751–758. [PubMed: 14688241]
19. Schroeder SJ, Blaha G, Moore PB. *Antimicrob. Agents Chemother* 2007;51:4462–4465. [PubMed: 17664317]
20. Wilhelm JM, Jessop JJ, Pettitt SE. *Biochemistry* 1978;17:1149–1153. [PubMed: 656379] Wilhelm JM, Pettitt SE, Jessop JJ. *Biochemistry* 1978;17:1143–1149. [PubMed: 656378] Böttger EC, Springer B, Prammananan T, Kidan Y, Sander P. *EMBO Rep* 2001;2:318–323. [PubMed: 11306553]
21. Kostrub, CF.; Diokno, R.; Aggen, JB.; Miller, GH.; Judice, JK.; Tulkens, PM. 19th European Congress of Clinical Microbiology and Infectious Diseases; Helsinki, Finland: Blackwell Publishing; 2009.

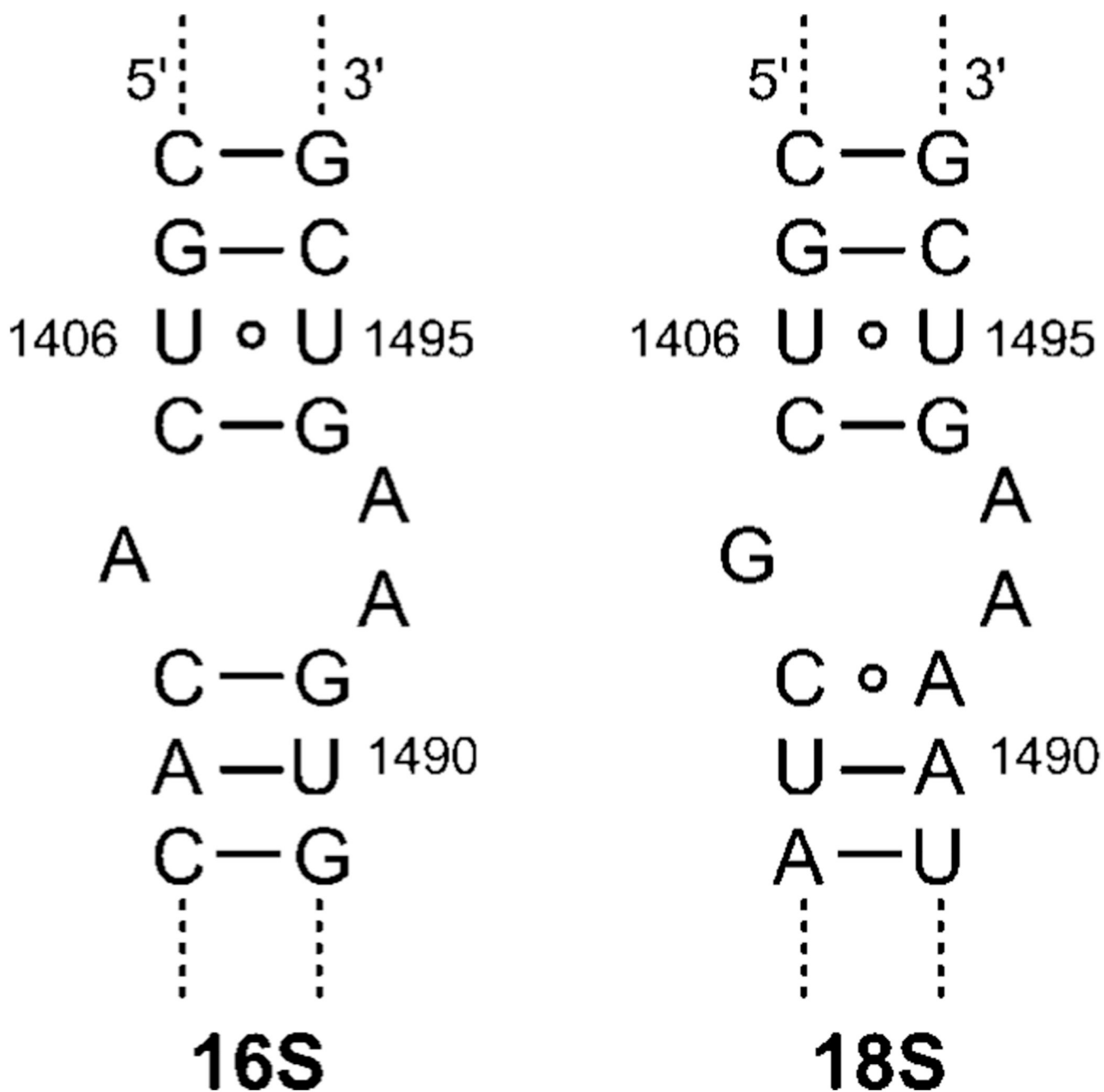


Fig. 1.
Sequences of the bacterial (16S) and human (18S) A-sites.

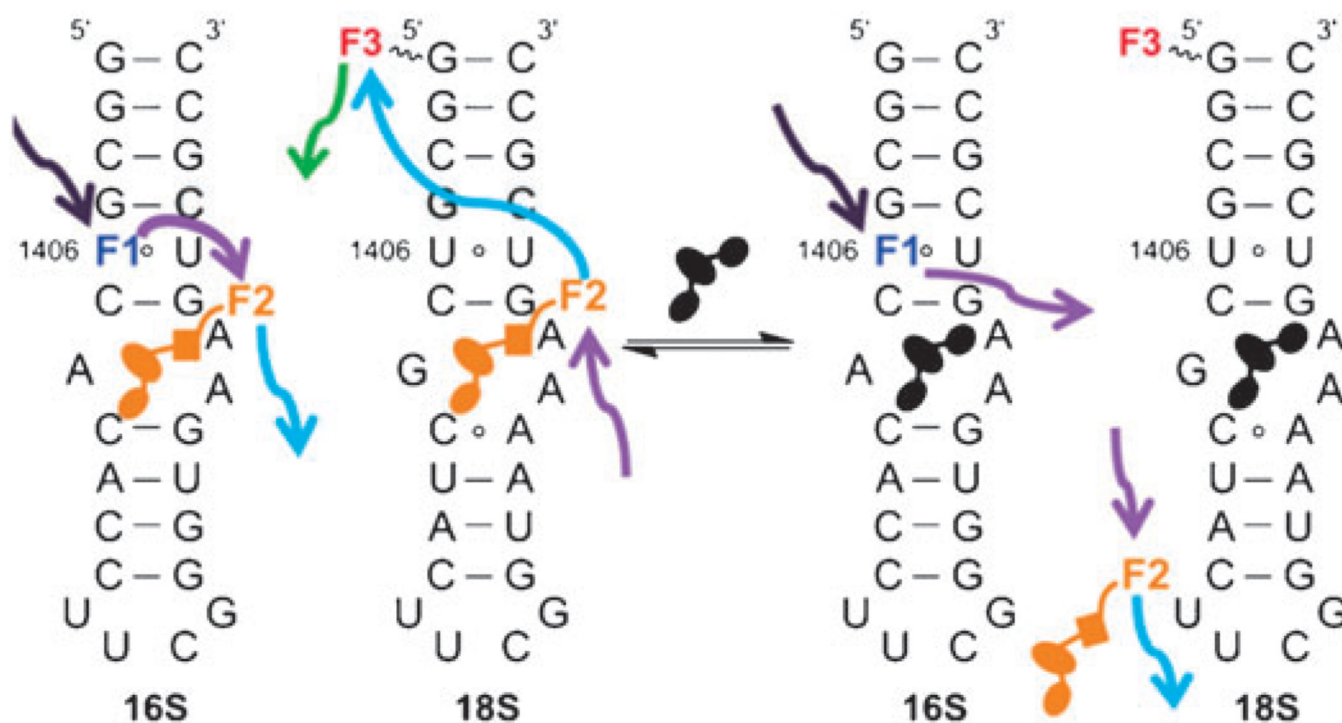


Fig. 2. Secondary structures for the 27-base RNA models of the 16S and 18S A-sites. U1406 of the 16S A-site is replaced with an isosteric emissive nucleoside analogue as a donor (**F1**); the place-holding molecule is tagged with an appropriate fluorophore (**F2**); the 18S A-site is tagged with an acceptor (**F3**) to match the labeled “place-holder” (**F2**). The affinity and selectivity of unlabeled small-molecules for either A-sites can be accurately monitored using FRET, as the place-holder is displaced.

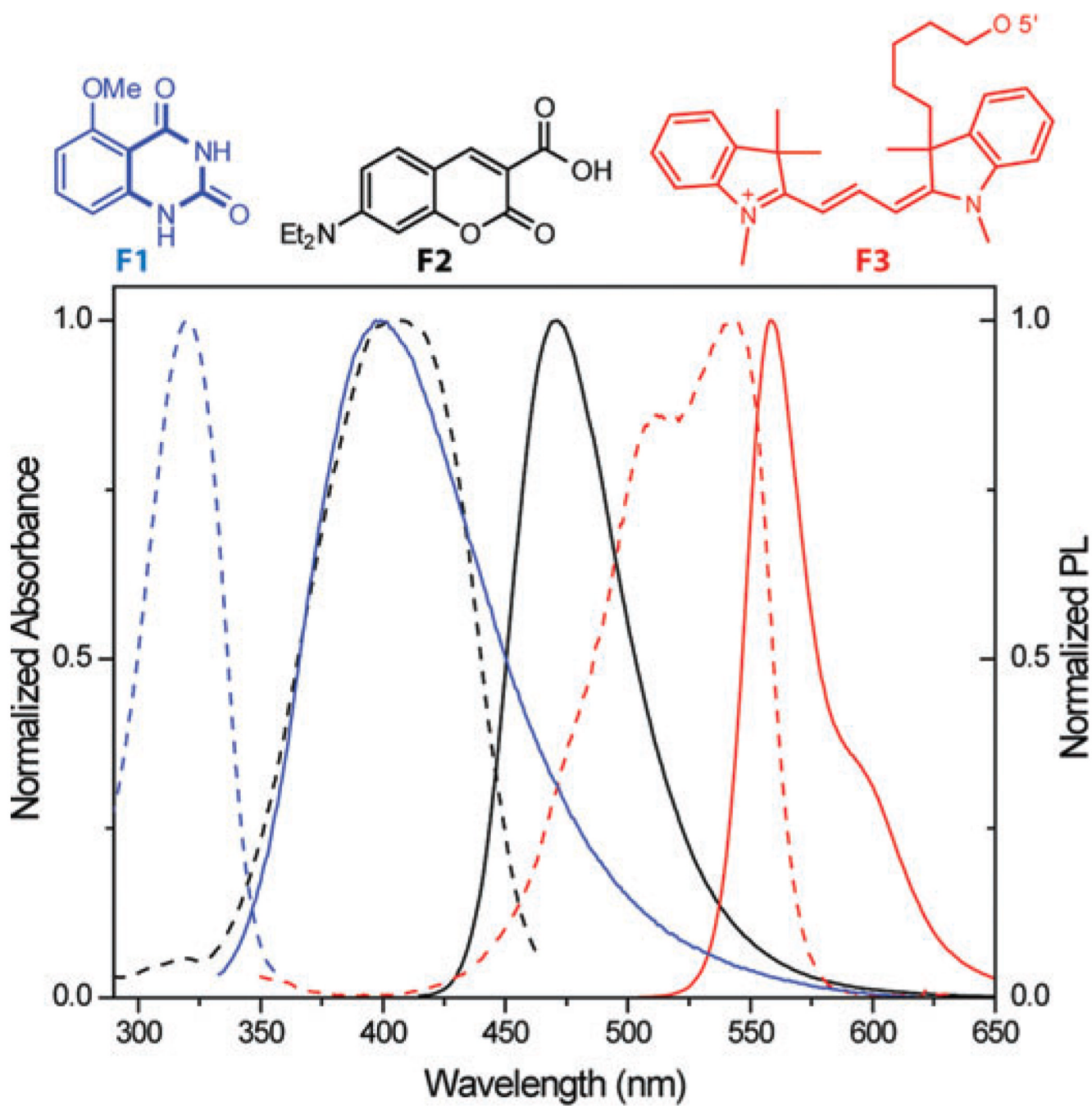


Fig. 3. Structures of **F1** (blue), **F2** (black), and **F3** (red) along with their normalized absorption (---) and emission spectra (—) in water.

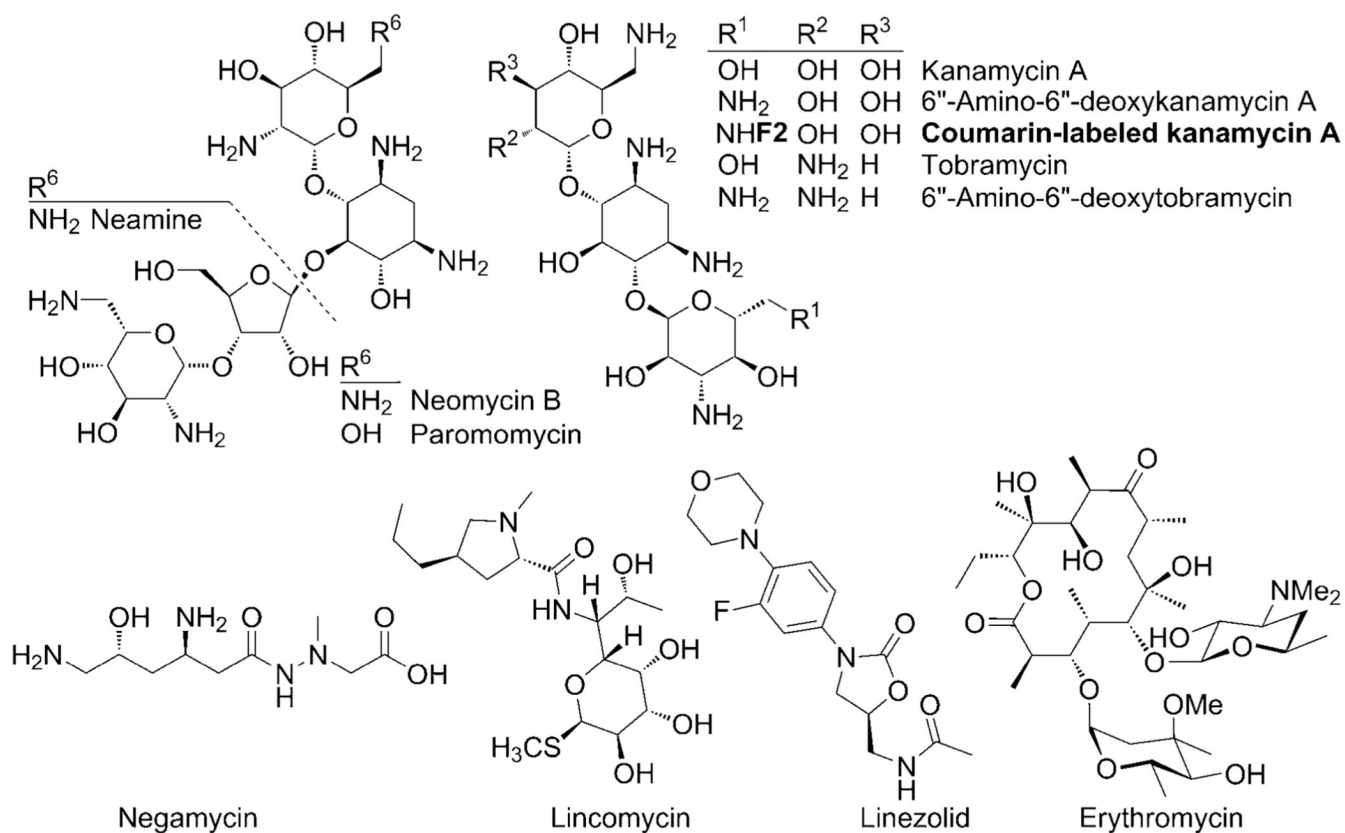


Fig. 4.
rRNA targeting antibiotics studied.

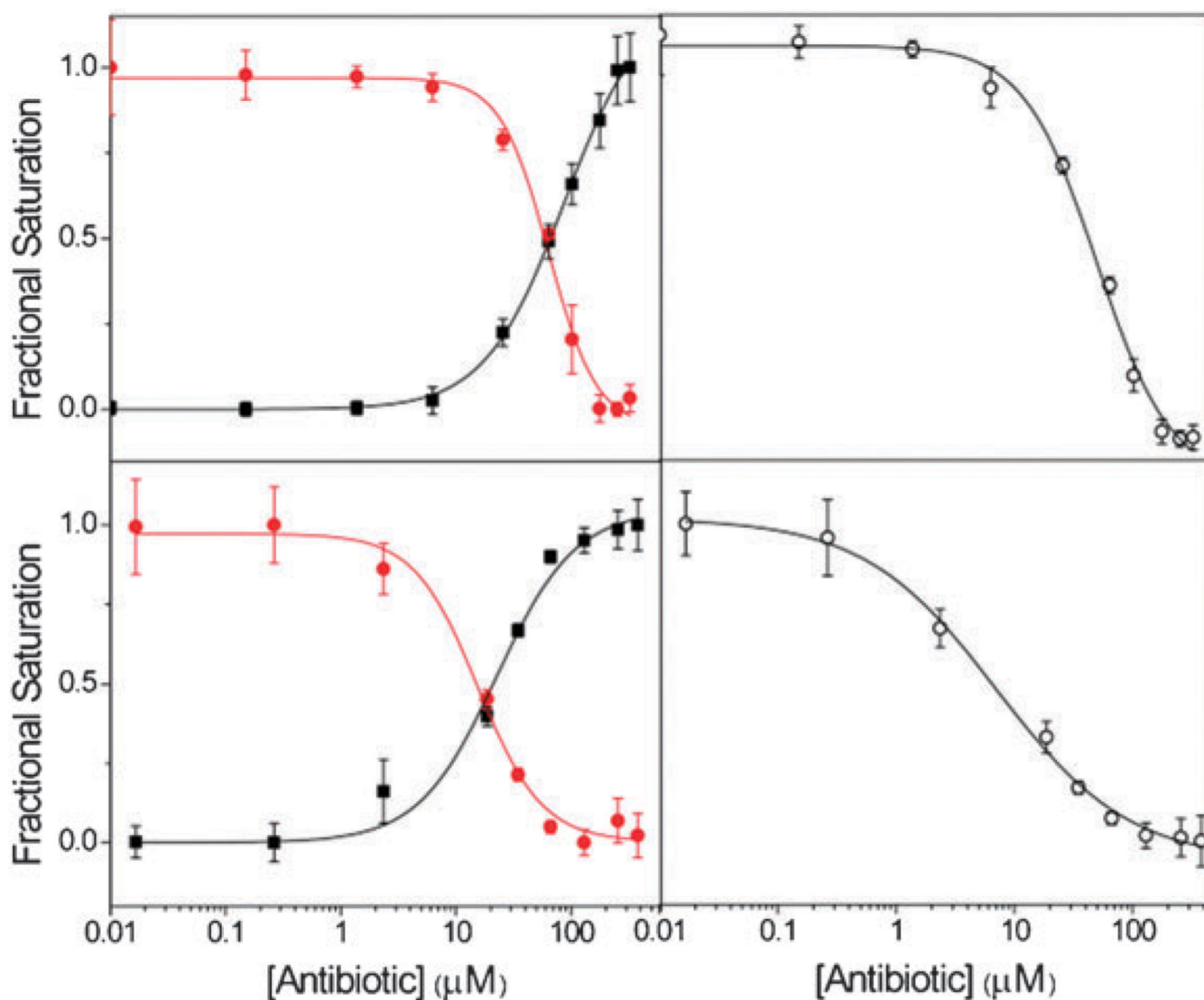


Fig. 5. Fractional fluorescence saturation of the donor **F1** (■) in the labeled 16S A-site, the emissive fluorophore **F2** (●) tagged to kanamycin A, and the emissive acceptor **F3** (○) of the 18S A-site in studying the binding of: (top) negamycin; (bottom) neamine. Conditions: 16S RNA (5×10^{-7} M), 18S RNA (5×10^{-7} M), coumarin-labeled-kanamycin A (2.2×10^{-6} M), cacodylate buffer pH 7.0 (2.0×10^{-2} M), NaCl (1.0×10^{-1} M).¹³

Table 1IC₅₀ values of antibiotics for the 16S and 18S A-sites^a

Antibiotics	16S A-Site/ 10 ⁻⁶ M	18S A-Site/ 10 ⁻⁶ M	Selectivity ratio
Neomycin B	2.8 (± 0.3)	4.7 (± 0.2)	0.60
Tobramycin	20.2 (± 0.4)	19.5 (± 0.3)	1.0
Paromomycin	9 (± 1)	8.0 (± 0.6)	1.1
Kanamycin A	75 (± 3)	46 (± 2)	1.6
Amino-tobramycin	4.2 (± 0.4)	3.8 (± 0.4)	1.1
Amino-kanamycin A	11.9 (± 0.4)	4.7 (± 0.3)	2.5
Negamycin	62 (± 5)	42 (± 3)	1.5
Neamine	18 (± 2)	6 (± 1)	3
Erythromycin	1880 (± 10)	1750 (± 10)	1.1
Lincomycin	> 8.5 × 10 ³	> 8.5 × 10 ³	—
Linezolid	> 9.6 × 10 ³	> 9.6 × 10 ³	—

^a Conditions as listed in Fig. 5.